SAJCCE 1:1 (2015) 1-24 October 2015
ISSN: 2394-2258
Available at http://scientificadvances.co.in
DOI: http://dx.doi.org/10.18642/sajcce_7100121440

AN EXPERIMENTAL STUDY ON PERFORMANCE OF REINFORCED CONCRETE COLUMNS WITH STRUCTURAL DEFICIENCY

V. Zanjani Zadeh[a] **and S. Eshghi**[b]

[a]Department of Civil, Construction and Environmental Engineering, North Carolina State University, Campus Box 7908, Raleigh, NC, 27695-7908, USA

[b]International Institute of Earthquake Engineering and Seismology (IIEES), Tehran, Iran

Abstract

Cyclic performance of slender reinforced concrete (RC) columns with insufficient lap splice length enclosed by widely-spaced transverse bars with 90-degree hooks is studied in this paper. Four half-scale RC columns with 150mm square cross section and 1000mm height fixed in strong foundation were tested under reversed cyclic loading and different constant axial load levels. Three specimens were built accordance with ACI (pre-1971), and one specimen was built according to ACI (318-02) provision to serve as a benchmark. Plastic hinge method was also used to calculate flexural deflection of the columns. The results demonstrated that poorly confined short lap splices in the potential plastic hinge region of a slender column can result in significant reduction in ductility and strength. Hysteretic loops for the columns were unstable with rapid degradation of strength and pinching effect due to premature splice failure. High axial load resulted in considerable reduction in the ductility and energy dissipation capacity of the columns. In general, it seems the common mode of failure for the specimens was the bond deterioration of the spliced longitudinal reinforcements.

*Corresponding author.
E-mail address: vzanjan@ncsu.edu (V. Zanjani Zadeh).

Submitted by S. Naganathan.
Received January 12, 2015; Revised January 28, 2015

Keywords: reinforced concrete columns, lap splice length, hysteretic loop, ductility, strength.

Nomenclature

P : Axial force.

$f_c^{'}$: Compressive strength of the concrete.

A_g : Gross cross-sectional area.

A_{sh} : Lateral reinforcements area.

ρ_{sh} : Lateral reinforcement ratio.

M_p : Measured flexural strength.

M_u : Theoretical flexural strength.

Δ : Total flexural deflection.

Δ_e : Elastic flexural deflection.

Δ_P : Plastic flexural deflection.

I_g : Gross moment of inertia.

I_e : Effective moment of inertia.

b : Width of column cross section.

d : Height of column cross section.

L : Column height.

L_p : Length of the plastic hinge.

φ_e : Elastic curvature.

M : Bending moment right above plastic hinge.

M_n : Nominal bending moment capacity of the column.

E : Represents elastic modulus of the column.

d_{lb} : Bar diameter.

f_y : Yield strength of the longitudinal bars.

ε_c : Compressive post-yield strain of the concrete in extreme fiber.

ε_s : Steel strain in tension.

ϕ_P : Plastic curvature of the concrete.

θ_p : Rotation in the hinge region.

c : Depth of the natural axis.

1. Introduction

Columns are important for the structural integrity of buildings. Failure of column can lead to total or partial collapse of buildings during major seismic actions (Moehle et al. [1]). Buildings that were constructed before the 1970s can have significant deficiencies in their overall structural configuration and detailing. The 1971 San Fernando earthquake, and the earthquakes that followed, demonstrated the vulnerability of columns during major seismic events and showed that during an earthquake columns are the most vulnerable component of a building. The longitudinal bars were used to be spliced with the lap length of 20-times of longitudinal bars diameters independent of column size, strength, or deformation demands. Besides, the often small-diameter transverse reinforcement was typically located widely, with 90-degree bends for anchorage. These columns were generally deficient in two respects: low transverse steel causing either premature shear failures or small ductile response, and short lap spliced longitudinal bars located immediately above the floor or foundation of the columns causing premature bond failure (Lynn et al. [2]).

In many countries with high seismic activities, numerous RC frame structures exist that were designed and constructed conforming to earlier codes without seismic loads consideration. Many of the construction details used in the structures are now recognized to be associated with non-ductile failure modes when subjected to seismic excitement (Eshghi & Zanjanizadeh [3, 4]). As a result, they are vulnerable against moderate to severe earthquakes. In addition, due to poor construction practice and inspection in some countries, yet defective and flaw detailing has been implementing without meeting seismic demands. Furthermore, information gathered from past earthquakes demonstrates that there is a significant gap between requirements established by modern seismic codes and construction practices especially in rural areas. As a consequence, flaws in design, and/or construction practices can bring about same detailing deficiency, similar to ACI (pre-1971) provision, even in recently built structures. In addition to these flaws if these columns are slender, for example due to certain architectural intervention in the first floor to have higher ground story which can lead to soft story mechanism or sever damages as reported in past earthquakes (e.g., Figure 1), they will be more vulnerable, e.g., (Inel et al. [5]; Kaplan et al. [6]).

Figure 1. Slender columns and large permanent inelastic deformation (Wenchuan, China, 2008) [Source: RMS].

Figure 2 and Figure 3 show damaged two columns due to lap splice deficiency and lack of confinement in plastic hinge zone. Figure 3 reveals that such detailing deficiency can cause severe damage in a RC building. These observations from recent earthquakes also show that columns with such detailing deficiency still exist; therefore, understanding the behaviour of these columns is an important matter.

Figure 2. Damage in lap splice zone caused by absence of adequate confinement and improper splice (Bio-bio, Chili, 2010) [Source: RMS].

Figure 3. Collapsed RC column due to inadequate lap splice length and widely-spaced transverse bars (Kashmir, Pakistan, 2005) [Source: RMS].

There is relatively little research on the behaviour of RC columns with deficient lap splices. Early works examined mostly the rehabilitation options for splices. Valluvan et al. [7] conducted experiments on columns subjected to pure tension. Aboutaha et al. [8]

carried out research on columns subjected to uniaxial bending with no superimposed axial load. Melek & Wallace [9] assessed the cyclic behaviour of typical RC building columns built according to ACI (pre-1971). In addition, some researchers studied the rehabilitation measures for bridges columns with such structural deficiency, by adding external and internal ties, as well as the use of FRP and steel jackets, e.g., (Chai et al. [10]; Aboutaha et al. [8]; Xiao & Ma [11]; Seible et al. [12]; Chang et al. [13]; Eshghi & Zanjanizadeh [14]; Harajli [15]; and ElGawady et al. [16]). Several researches were focused on analytical and numerical modelling of such columns, e.g., (Chowdhury et al. [17]; Zanjanizadeh & Eshghi [18]). Although slender RC columns are popular in earthquake prone areas, less research exists on performance these columns with poor lap-splice detail and normal strength concrete. A small number of studies investigated the strengthening of slender columns without such detailing deficiency, e.g., (Tao & Yu [19]; Gajdošová & Bilèík [20]), and with high-strength concrete, e.g., (Claeson & Gylltoft [21]; Pallarés et al. [22]). The lack of knowledge on the cyclic load performance of slender building columns with poor splice detailing brings about uncertainty for seismic rehabilitation of such columns. Thereby knowing the response of these columns to earthquake is of particular importance in order to aid researchers to innovate new techniques to remedy these deficiencies and achieve the acceptable performance level.

This paper describes the experimental results from a research program designed to investigate the hysteretic behaviour of slender RC columns with poor lap-spliced longitudinal reinforcement detail. The columns were tested under low axial force and large bending moments, as slender columns are especially more susceptible to this type of loading. Plastic hinge method was also used to calculate flexural deflection of the columns.

2. Experimental Program

2.1. Specimen geometry and reinforcing layout

Four half-scale ground floor column specimens were constructed to investigate performance of slender RC columns with lap splice detailing deficiency. All the columns had the square cross section of 150 × 150mm and 1000mm height with a 350 × 550 × 350mm foundation block in order to provide full anchorage. The reinforcing details of the specimens were different. SP1, SP2, and SP3 were reinforced by eight 8mm longitudinal deformed bars which enclosed by 4mm ties with 90-degree hooks spaced at 160mm throughout the column to comply with ACI (pre-1971) provisions. The lap splice length was 160mm (20 bar diameters). However, SPC4 was built accordance with ACI (318-02) provisions, and had eight 8mm deformed longitudinal bars with 320mm lap splice length enclosed by 4mm ties with 135-degree hooks at 60mm. All the specimens were slender $(\frac{L}{d} > 11)$ to represent specific classification of columns which exist in high-seismic regions.

2.2. Material properties

The specimens were cast using mixed concrete with water/cement ratio of (0.45). Maximum size of the limestone was 15mm. Ordinary port land cement was employed in the mixture. The columns and foundations were cast vertically and integrally, and vibrated with a vibrator rod to release the entrapped air voids. Six standard concrete cylinders were tested (152mm diameter and 305mm height) to establish the mean compressive strength of the concrete. The average compressive strength at 28 days was 18.9MPa, whereas it was 19.8MPa at the time of testing the columns. Tension test was performed on steel bars to establish stress-strain relationship of steel reinforcing used as longitudinal and transverse reinforcement. The yield strength of M8 steel bar and M4 wire were 400MPa and 300MPa, respectively.

2.3. Applied loading

The cantilever specimens were subjected to combined shear cyclic displacement and constant axial loading at top level as shown in Figure 4. Axial load was applied using a 100kN capacity hydraulic jack through hinges at the ends of the specimens allowing in-plane end rotations. During testing, the axial load was maintained constant by the hydraulic system. The reversed cyclic displacement was applied through a servo-controlled actuator having 60kN load and ±60mm stroke capacities. Displacement control mode of the actuator was used to apply the predetermined displacement history. Axial load levels were approximately 5%, 10%, and 15% of the assumed column gross axial capacity $(A_g f_c')$ for SP1, SP2, and SP3, respectively.

Table 1. Specimen specifications and loading characteristics

Specimen	$P/f'cA_g$	Axial load(kN)	A_{sh}	ρ_{sh}%	Splice $(20\,d_b)$
SP1	0.05	21.2	0.112	0.258	No
SP2	0.10	42.4	0.112	0.258	Yes
SP3	0.15	63.6	0.112	0.258	Yes
SP4	0.05	21.2	0.112	0.644	Yes

The lateral reverse cyclic displacement was imposed on each of the following peak drift ratios: 0.25%, 0.5%, 0.75%, 1%, 1.25%, 1.5%, 1.75%, 2.25%, 2.75%, 3.25%, 3.75%, 4.25%, 4.75%, 5.25%, and 5.75% as the displacement increments with two cycles at each level of drift ratio. As displayed in Figure 4, to provide cantilever-type loading condition, the bottom stub of the specimens was fixed to the base in order to achieve full fixity.

Figure 4. General view of the test set up.

The longitudinal and transverse reinforcing bars and concrete of the specimens were instrumented with strain gauges to determine the steel and concrete strains at various locations and steps of the tests. Displacements were measured during testing by three linear variable differential transducers (LVDTs) (at the top, mid-height, and bottom of the columns), while the force response of the specimen was also continuously recorded. Also, two LVDTs were mounted on reaction wall and columns foundation to measure the possible uplift.

3. Test Results

3.1. Visual assessment of damage

The crack and failure patterns of each column at end of the test are shown in Figure 5. During testing of specimen SP-S1, initial flexural cracks were observed at the base of the column when displacement reached 1% of the drift ratio, and at 1.5% drift ratio at the end of the splice length. Some flexural cracks appeared along the splice during the test but the length and width of these cracks did not increase significantly.

Generally, similar damage was noticed in SP1, SP2, and SP3, that is, initially flexural cracking at the column-footing interface followed by horizontal cracks throughout the columns as the displacement increased. However, crack pattern changed to complex patterns thereafter including flexure, cover-concrete spalling, and shear cracks appearing near the ultimate load level. Cover spalling was an indication of splice failure in these columns (Melek & Wallace [9]). It seems that splitting bond failure induced cover-concrete spalling along the splice length in all these specimens. By increasing axial load the cracks appeared later and they were impulsive, and damage became more severe.

(a) SP1 (b)SP2 (c) SP3 (d) SP4

Figure 5. Failure modes and developed cracks of column specimens at end of the test.

3.2. Hysteretic response

Figure 6 presents the moment versus curvature response of the specimens. The total moment at interface was the sum of the primary moment produced by the lateral load plus the secondary moment caused by the axial load. The deflected shape of the column obtained from the LVDTs readings was used to compute the secondary moment. The differential rotation angle was measured as angle made by the tangent at the column-stub interface with the tangent drawn at the column tip. The deflection values obtained from the LVDTs were used to compute the rotation angle. The measured flexural strength of each specimen is also compared with its own theoretical strength (Mu). Theoretical strength (Mu) of the columns was calculated by using formula reported by Penelis & Kappos [23] and was found to be about 25KN-m. It is apparent from the hysteresis curves that the theoretical strength is always slightly less than the measured flexural strength for all the specimens. This is consistent with results reported by Xiao and Ma [11].

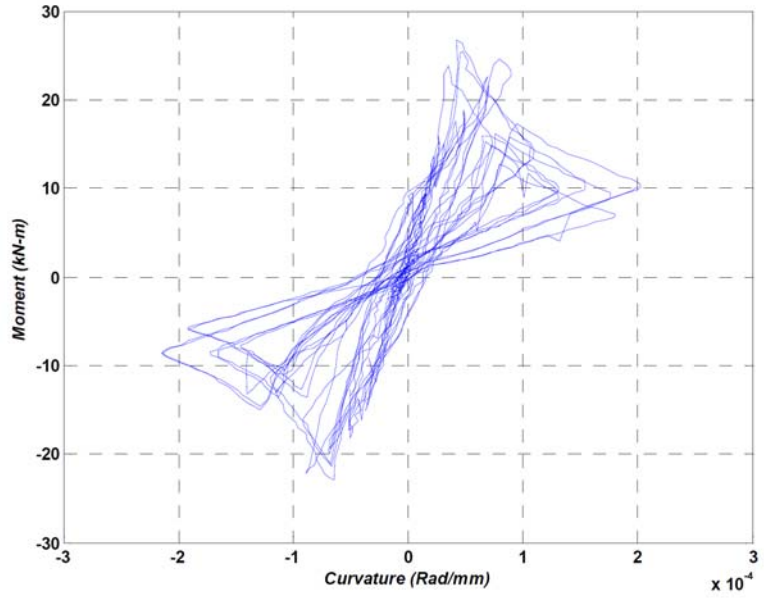
Moment (kN-m)
Curvature (Rad/mm)
x 10^-4

(a) SP1

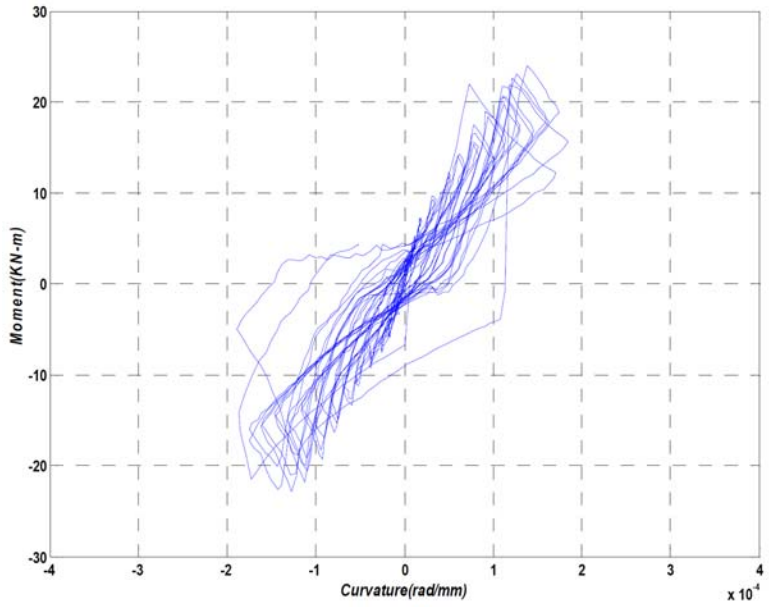
Moment(KN-m)
Curvature(rad/mm)
x 10^-4

(b) SP2

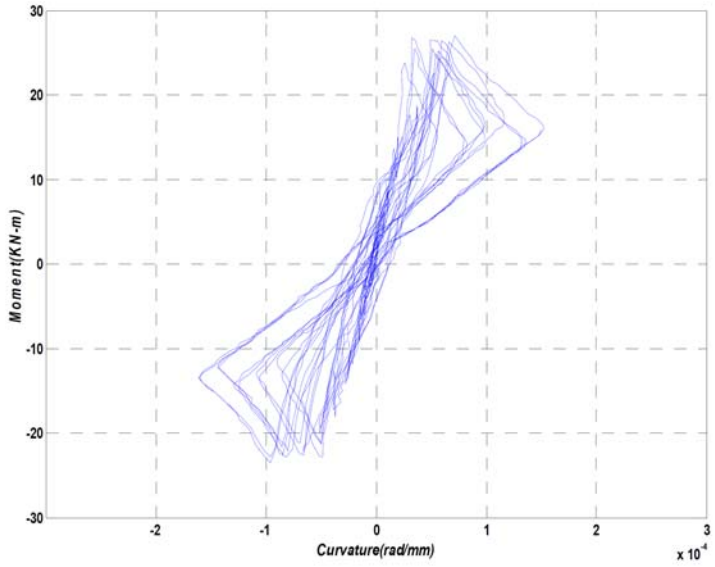

(c) SP3

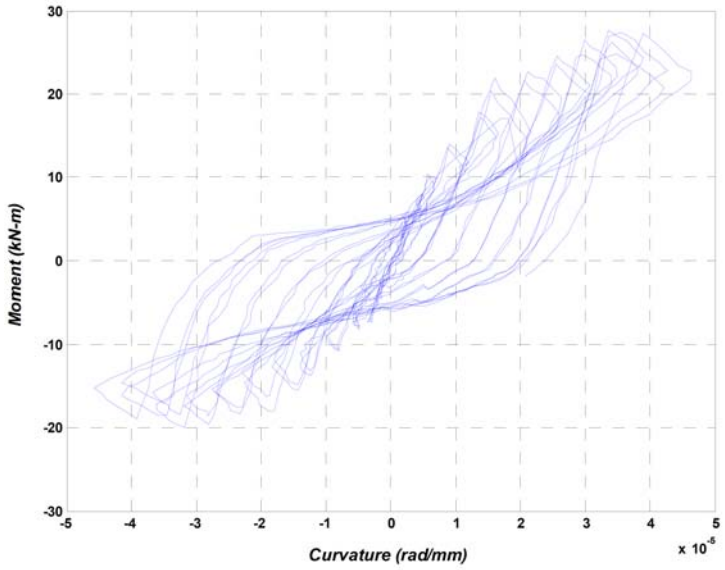

(d) SP4

Figure 6. Moment versus curvature curves of the specimens.

SP1, SP2, and SP3 attained their maximum moment capacities prior to 10^{-4} Rad/mm just before the concrete compression crush took place, irrespective of the level of axial load, whereas; SP4 reached its maximum moment capacity between 3×10^{-4} Rad/mm to 4×10^{-4} Rad/mm. The drift ratio at which these specimens attained the maximum measured moment is about ±1%, indicating a similar initial elastic stiffness for these specimens. For the columns built according to ACI (pre-1971), a gradual degradation in strength occurred shortly after attaining the peak load. This difference in the hysteretic performance is related to the lack of insufficient confinement and short lap splice. Overall, SP4 demonstrated a more stable response in the entire loading displacement range tested as a result of proper splicing and confinement detail compared to the columns were built according to ACI (pre-1971). A relatively good feature of the specimens is the large area contained in the hysteretic loops, indicating significant energy dissipation during testing. As shown in Figure 4 specimens with less axial load have more stable hysteretic curves due to second order effects; also, rapid stiffness degradation and pinching effect in SP1, SP2, and SP3 are obvious. Although the lateral confinement has little effect on strength enhancement of the columns, it enhanced the column ductility. It is important to note that, the effect on hysteresis loops were narrower and the pinching effect was much more severe than non-slender RC columns results reported by Wallace & Melek [9] and ElGawady et al. [16].

3.3. Residual displacement

Response of the RC columns to cyclic displacement is strongly dependent on the capability to sustain large inelastic deformation without significant load carrying capacity loss. Loss of load carrying capacity in structures can be obtained by measuring permanent displacement. This factor has important role in stability of buildings after earthquake. In particular, the magnitude of residual displacement is critically important in determining the technical and economic feasibility

of repairing damaged structures. In current research, large cyclic loading led to permanent residual displacements in the columns as summarized in Figure 7. Comparison of this deflection among the columns explains load carrying capacity loss of the each column. The indicated residual displacements correspond approximately to 12%, 16%, 20%, and 8% of maximum drifts for SP1, SP2, SP3, and SP4, respectively. Loss of load carrying capacity of the SP4 was the least between all the columns. In addition, there is a direct correlation between magnitude of axial force and load carrying capacity loss; the higher the axial load, the higher the load carrying capacity loss.

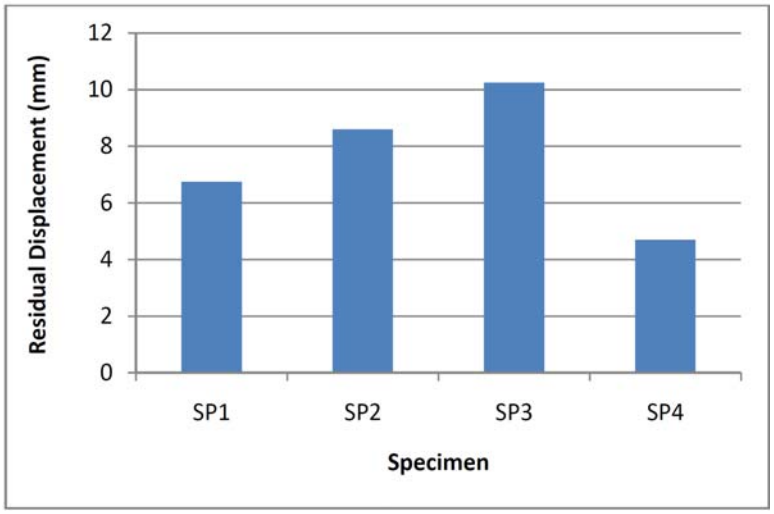

Figure 7. Residual displacement of the samples after test.

3.4. Total energy dissipation

Total dissipated energy during cyclic loading of a structural system is a useful measure that represents its performance when subjected to earthquake excitation, has been recognized by many researchers, e.g., (Park et al. [24]). In general, fuller hysteresis loops means higher seismic energy removal from the structure, which is logically implies better performance when comparing systems with similar strength. Total

dissipated energy was calculated for each column from moment-curvature hysteretic curves and shown in Figure 8. Dissipated energy at each cycle was calculated by taking the area under each loop of moment-curvature curves, and cumulating whole enclosed areas of the cycles. As indicated, SP4 dissipated almost 52% more total energy than SP1. Also, as the axial load increases the total dissipated energy is decreased. SP1 dissipated twice and three times more than SP2 and SP3, respectively. Since imposed drift ratios were numerous and high, high energy dissipation was observed.

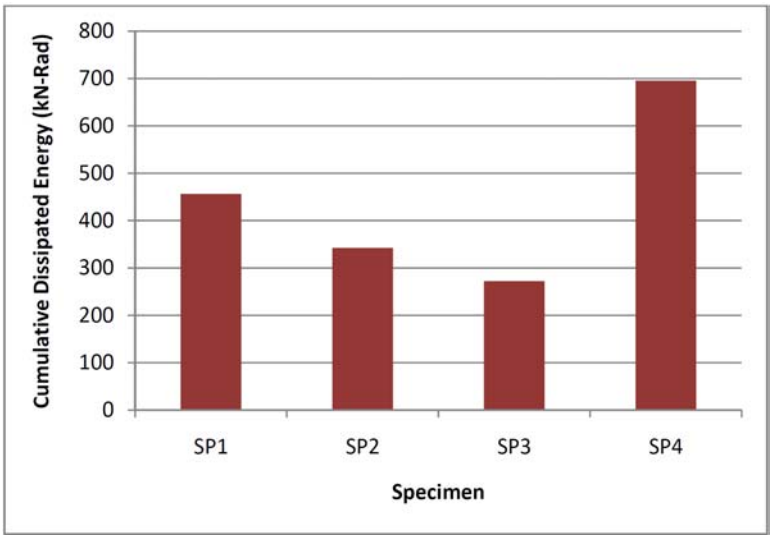

Figure 8. Total dissipated energy for the samples.

4. Plastic Hinge Method to Calculate Flexural Deflection

One of the popular methods to calculate the flexural deflection of an RC member is the plastic hinge method. This method could be used to estimate key deformation characteristics of RC columns deflection including: plastic rotation, plastic curvature, and plastic strain in different drift ratios. In this section, plastic deformation characteristics of the columns specimens were calculated using plastic-hinge method adopted from two PEERC reports (Esmaeily-Gh & Xiao [26]; Berry &

Eberhard [25]). According to this method, the total deformation is divided into elastic and plastic parts and is expressed as

$$\Delta = \Delta_e + \Delta_P, \tag{1}$$

where Δ_e and Δ_P are the elastic and plastic flexural deflection, respectively. This deflection may either be computed exactly based on either the moment-curvature relationship or the assumption that the curvature distribution within the yield curvature is linear. Computing of the elastic flexural deflection is on order of

$$I_g = \frac{bd^3}{12}, \tag{2}$$

$$I_e = 0.7 I_g, \tag{3}$$

$$M_y = \left(\frac{L - L_p}{L}\right) M_n, \tag{4}$$

$$\phi_e = \frac{M}{EI}, \tag{5}$$

$$\Delta_e = \frac{\phi_e (L - L_p)^2}{3}, \tag{6}$$

where I_g and I_e are gross and effective moment of inertia, respectively; b and d are width and height of column cross section, respectively; L is the column height, and L_p denotes the length of the plastic hinge; φ_e is the elastic curvature; M is the bending moment right above plastic hinge, and M_n is the nominal bending moment capacity of the column; and E represents elastic modulus of the column. In this study, the plastic hinge formulation of Priestly and Park was employed. In order to obtain both elastic and plastic deformation, plastic hinge length is needed. Priestley and Park [27] proposed a plastic hinge length that considers the full development of the columns longitudinal reinforcements into the footing, and depends on the rebar diameter and column length. The proposed plastic hinge length is

$$L_P = 0.08L + 0.022d_{Ib}f_y, \tag{7}$$

where d_{Ib} denotes the bars diameter and f_y is the yield strength of the longitudinal bars. Figure 9 is a typical illustration of the plastic hinge method introduced by Priestley and Park [27]. Using Equation (7), the length of the plastic hinge region will be 140mm for the columns.

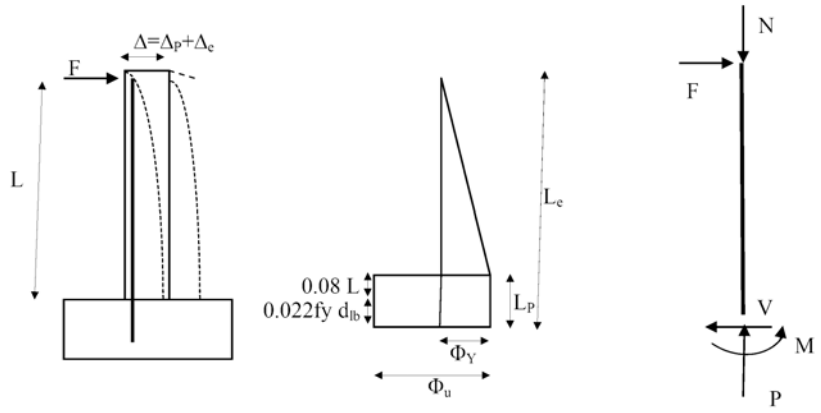

Figure 9. Plastic hinge analysis parameters (Priestley & Park [27]).

Δ_P in Equation (1) is the post-yield deflection resulting from the plastic hinge and is computed as follows:

$$c = \frac{\varepsilon_c}{\varepsilon_c + \varepsilon_s} d, \tag{8}$$

$$\phi_P = \frac{\varepsilon_c}{c}, \tag{9}$$

$$\theta_P = \phi_P \times L_P, \tag{10}$$

$$\Delta_P = \theta_P \times (L - L_P / 2), \tag{11}$$

where ε_c = compressive post-yield strain of the concrete in extreme fiber; ε_s = steel strain in tension; d = distance from extreme compression fiber to centroid of tension reinforcement; ϕ_P = plastic curvature of the concrete; θ_P = rotation in the hinge region; and c = depth of the natural axis.

Figure 10 and Figure 11 show concrete strain and plastic curvature of the specimens in different drift ratios, respectively. Lowest concrete strain and plastic curvature was occurred in SP1. Concrete stain increases as the axial loading increases. Although this is consistent with experimental observation, it does not represent the actual response of slender columns to cyclic loading. In experimental study, the columns with short lap splice sustained more severe damage than one with sufficient lap splice. Also, even for SP1 which was built according to modern ACI provision, the plastic curvature was 30-40% greater than the ones were recorded in the experiments. This difference can be partly attributed to slenderness of the experimental columns that is ignored in plastic hinge method.

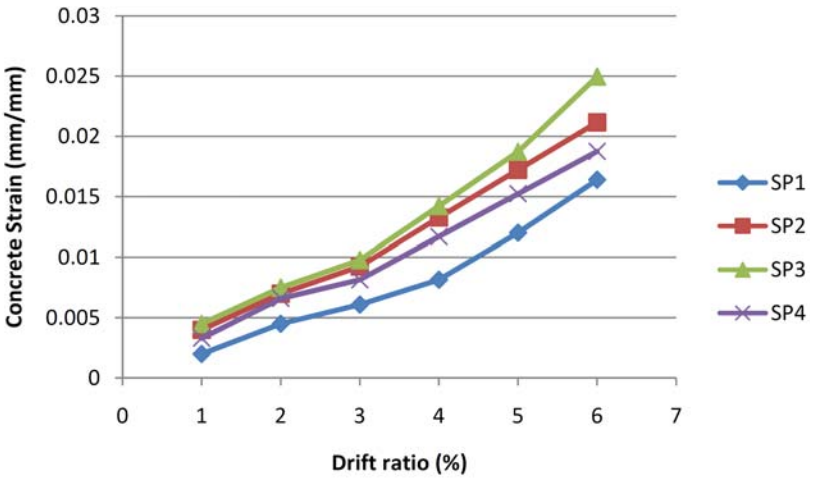

Figure 10. Strain in concrete in different drift ratios.

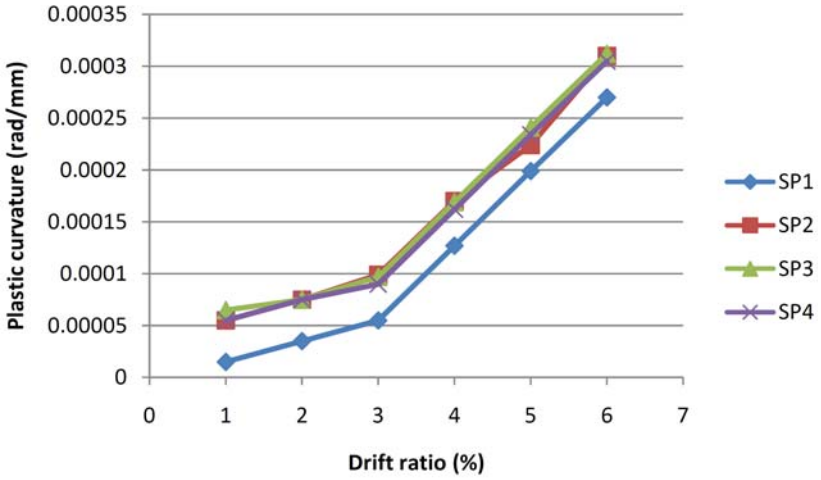

Figure 11. Plastic curvature in different drift ratios.

5. Conclusion

The effects of poor lap splice detailing on strength and ductility of slender RC columns has been investigated experimentally. Four slender RC column specimens, which detailed with short lap splices and inadequate transverse confinement reinforcement with 90-degree hooks in the potential plastic hinge zone near footing-column joints, characteristic of pre-1971 design provision, were tested under low to moderate level of compressive axial load $(P/A_g f_c \approx 0.05 - 0.15)$ and reversed cyclic inelastic displacement. All in all, it is concluded that such columns suffer from brittle failure when they subject to lateral cyclic loading. In order to estimate the capacity of these columns, accurate modelling of their lap splice and confinement detail is essential. The following conclusions also can be drawn from this study:

(1) From the test results, it is evident that the presence of poorly detailed lap splices in the potential plastic hinge region of a slender column leads to significant ductility reduction as well as unstable hysteretic behaviour with rapid degradation of strength and pinching effect due to premature splice failure.

(2) SP1 has the most stable hysteretic response. This could be due to yielding the longitudinal reinforcing bars without shear or splice failure.

(3) High axial load resulted in considerable reduction in the ductility and energy dissipation capacity of the columns.

(4) The plastic hinge method results approximately were in agreement with experimental work; however, induced concrete strain in the method was much lower than experimental one, which it could be attributed to the lap splice failure in the specimens. The contribution of bond-slip in the splice region to lateral displacements can be substantial and should not be ignored in the analysis of older RC construction. For the cantilever columns studied here, the bond-slip effects were computed to account for about 30% of the calculated lateral curvature corresponding to the peak load.

References

[1] J. P. Moehle, W. Ghannoum and Y. Bozorgnia, Collapse of lightly confined reinforced concrete frames during earthquakes, in: S. T. Wasti and G. Ozcebe (Eds.), Advances in Earthquake Engineering for Urban Risk Reduction, Nato Science Series: IV: Earth and Environmental Sciences, Springer Netherlands, (2006), 317-332.

[2] A. C. Lynn, J. P. Moehle, S. A. Mahin and W. T. Holmes, Seismic evaluation of existing reinforced concrete building column, Earthquake Spectra 12(4) (1996), 715-739.

[3] S. Eshghi and V. Zanjanizadeh, Repair of earthquake-damaged square R/C columns with glass fiber-reinforced polymer, International Journal of Civil Engineering 5(3) (2007), 210-223.

[4] S. Eshghi and V. Zanjanizadeh, Cyclic Behavior of Slender R/C Columns with Insufficient Lap Splice Length, 14th World Conference on Earthquake Engineering, Beijing, China, 2008.

[5] M. Inel, H. B. Ozmen and E. Akyol, Observations on the building damages after 19 May 2011 Simav (Turkey) earthquake, Bulletin of Earthquake Engineering 11(1) (2013), 255-283.

[6] H. Kaplan, H. Bilgin, S. Yilmaz, H. Binici and A. Oztas, Structural damages of L'Aquila (Italy) earthquake, Nat Hazards Earth Syst. Sci. 10 (2010), 499-507.

[7] R. Valluvan, M. Kreger and J. Jirsa, Strengthening of column splices for seismic retrofit of nonductile reinforced concrete frames, ACI Structural Journal 90(4) (1993), 432-440.

[8] R. S. Aboutaha, M. D. Engelhardt, J. O. Jirsa and M. E. Kreger, Retrofit of concrete columns with inadequate lap splices by the use of rectangular steel jackets, Earthquake Spectra 12(4) (1996), 693-714.

[9] M. Melek and J. W. Wallace, Cyclic behavior of columns with short lap splices, ACI Structural Journal 101(6) (2004), 802-811.

[10] Y. H. Chai, M. J. N. Priestley and F. Seible, Seismic retrofit of circular bridge columns for enhanced flexural performance, ACI Structural Journal 88(5) (1991), 572-584.

[11] Y. Xiao and R. Ma, Seismic retrofit of RC circular columns using prefabricated composite jacketing, Journal of Composite for Construction 123(10) (1997), 1357-1364.

[12] F. Seible, M. J. N. Priestley, G. A. Hegermier and D. Innamorato, Seismic retrofit of RC columns with of RC columns with continuous carbon fiber jackets, Journal of Composite for Construction 1(2) (1997), 52-62.

[13] K. Chang et al., Seismic Retrofit Study of RC Bridge Columns, National Center for Research on Earthquake Engineering, Taiwan, 2002.

[14] S. Eshghi and V. Zanjanizadeh, Retrofit of slender square concrete columns by glass fiber-reinforced polymer for seismic resistance, Iranian Journal of Science and Technology 32(B5) (2008), 437-450.

[15] M. H. Harajli, Behavior of gravity load-designed rectangular concrete columns confined with fiber reinforced polymer sheets, Journal of Composites for Construction 9(1) (2005), 4-14.

[16] M. ElGawady, M. Endeshaw, D. McLean and R. Sack, Retrofitting of rectangular columns with deficient lap splices, Journal of Composites for Construction 14(1) (2009), 22-35.

[17] S. R. Chowdhury and Kutay Orakcal, Analytical modeling of columns with inadequate lap splices, ACI Structural Journal 110(5) (2013), 735-744.

[18] S. Eshghi and V. Zanjanizadeh, Finite element modeling of retrofitted reinforced concrete columns with glass fiber reinforced polymer, SHARIF: Civil Engineering 40 (2008), 21-28.

[19] Z. Tao and Q. Yu, Behaviour of CFRP-strengthened slender square RC columns, Magazine of Concrete Research 60(7) (2008), 523-533.

[20] K. Gajdošová and J. Bilèík, Slender reinforced concrete columns strengthened with fiber reinforced polymers, Slovak Journal of Civil Engineering 19(2) (2011), 2-6.

[21] C. Claeson and K. Gylltoft, Slender high-strength concrete columns subjected to eccentric loading, Journal of Structural Engineering 124(3) (1998), 233-240.

[22] L. Pallarés, J. L. Bonet, P. F. Miguel and M. A. Fernández Prada, Experimental research on high strength concrete slender columns subjected to compression and biaxial bending forces, Engineering Structures 30(7) (2008), 1879-1894.

[23] G. Penelis and A. J. Kappos, Earthquake-Resistance Concrete Structures, E & FN Spon Published, 1997.

[24] Y. J. Park, A. H. Ang and Y. K. Wen, Damage-limiting aseismic design of buildings, Earthquake Spectra 3(1) (1987), 1-26.

[25] M. Berry and M. O. Eberhard, Performance Models for Flexural Damage in Reinforced Concrete Columns, Pacific Earthquake Engineering Research Center, College of Engineering, University of California, 2004.

[26] A. Esmaeily-Gh and Y. Xiao, Seismic Behavior of Bridge Columns Subjected to Various Loading Patterns, Pacific Earthquake Engineering Research Center, College of Engineering, University of California, 2002.

[27] M. J. N. Priestley and R. Park, Strength and ductility of concrete bridge columns under seismic loading, ACI Structural Journal 84(1) (1987), 61-76.

■